Advances in Science and Technology Research Journal

Advances in Science and Technology Research Journal, 2025, 19(10), 461–474
https://doi.org/10.12913/22998624/208233
ISSN 2299-8624, License CC-BY 4.0

Received: 2025.06.06
Accepted: 2025.08.10
Published: 2025.09.01

Using artificial intelligence to optimize g-code files for fused filament fabrication/fused deposition modeling technology

Zbigniew Andrzej Pilch[1*], Maciej Gibas[1]

[1] Faculty of Electrical Engineering, Cracow University of Technology, ul. Warszawska 24, Kraków, Poland
* Corresponding author's e-mail: zbigniew.pilch@pk.edu.pl

ABSTRACT

3D printing technology – particularly thermoplastic-based methods such as fused filament fabrication (FFF) and fused deposition modeling (FDM) – has gained popularity in both industrial and home settings. A key element of the 3D-printing process is the preparation of the printer's batch files – so-called g-code files – which contain all the information needed for correct execution of the print. Traditional methods of generating g-code rely on deterministic algorithms that do not always yield optimal results in terms of print quality (dimensional accuracy of the geometry), build time, material consumption, and functional parameters such as the mechanical strength of the printed part. In recent years, interest has grown in using artificial intelligence (AI) to optimize these processes. AI algorithms, including machine learning and deep learning, have the potential to analyse and optimize g-code in ways that surpass traditional approaches, offering higher print quality, greater energy efficiency, and shorter production times. This work explores the modification of print parameters recorded in g-code files through the use of AI, demonstrating that the modified files produce prints with improved mechanical strength. A large language model (ChatGPT-4o) was used to selectively modify nozzle temperature parameters in g-code files, based on prompt engineering and filament datasheets. Tensile samples made from Easy PLA and Easy PET-G filaments were printed and tested in three-point bending, in accordance with ISO 14125. The samples were divided into three groups: unmodified (reference), modified every 2 layers, and modified every 3 layers. The results showed an increase in the average breaking force for PLA samples by 2.7% and 3.0%, and for PET-G samples by 4.3% and 9.9%, respectively. Comparative analysis of the g-code files confirmed that the AI introduced cyclic temperature changes (increase in M104 commands from 3 to 30), improving interlayer adhesion. The flexural strength improvements were consistent with these modifications. In conclusion, AI-driven g-code optimization offers a simple and effective way to improve the mechanical properties of printed objects without altering geometry or increasing material usage. This approach holds great potential for advancing additive manufacturing processes, particularly in the context of Industry 4.0.

Keywords: additive manufacturing ; FFF/FDM technology, AI, optymize g-code.

INTRODUCTION

3D printing technology – particularly methods such as fused filament fabrication (FFF) and fused deposition modeling (FDM) – has become increasingly popular in both industrial and home applications. A crucial element of the 3D printing process is the preparation of input files for the printer – so-called g-code files – which contain all the information necessary for the correct execution of the print. These files control and command the movements of the actuators responsible for nozzle positioning over the build area in the XYZ axes, the speed of the extruder mechanism, nozzle and bed temperatures, as well as many other critical printing parameters.

Traditional methods of generating g-code, implemented in so-called slicers, rely on deterministic algorithms that do not always lead to optimal results in terms of print quality [1, 2], build time, or material consumption [3, 4]. An interesting study is presented in [1], where the dimensional accuracy of a test part – compliant with the ISO 16792:2021-04 standard – was evaluated. The

dimensional fidelity of prints created using FDM, SLA, and SLS methods was compared against the original CAD model. In [2], the influence of printing speed on the surface quality of printed components was investigated. Other studies focus on the mechanical properties of prints depending on infill pattern [5], material type [6], nozzle diameter [5], or the temperature distribution within the printing zone [7].

In recent years, interest in the application of artificial intelligence (AI) to optimize these processes has grown significantly. AI algorithms, including machine learning and deep learning, have the potential to analyze and optimize g-code files in ways that surpass traditional approaches, offering improved print quality, enhanced energy efficiency, and reduced production time [8], [9], [10].

3D printing technology

The origins of 3D printing technology date back to the 1980s, when Charles Hull began work on this manufacturing method for the purpose of rapid prototyping [11]. A key milestone in the development of 3D printing was the creation of the STL file format (STereoLithography or Standard Tessellation Language) in 1983, which enabled communication between the 3D printer and the digital model. The first 3D printer was developed by Charles Hull and 3D Systems, and was named the Stereolithography Apparatus (SLA). The first commercial solution, called SLA 250, was introduced in 1988 [11].

In 1990, the FDM technique was developed by Scott Crump, and the first patent application for 3D printing technology was filed in 1993. In recent years, 3D printing technology has experienced rapid growth, with numerous companies entering the market to develop increasingly advanced, reliable, and functional devices, as well as materials used in the printing process. Additive manufacturing technologies currently developed and implemented can be divided into three main groups:

- Printing with thermoplastic filaments, shaped into strands of a specified diameter, which are fed into a print head that melts and deposits the material layer by layer. This group includes FFF/FDM methods.
- Printing with photosensitive resins, which are locally cured by a light source. The light source may be a laser beam (SLA), a projector lamp (DLP), or an LED array (LED method).
- Printing with powdered materials, including CJP (gypsum), SLS (plastics), and SLM (metal powders).

All 3D printing methods require proper preparation of digital models. The complete cycle from idea to finished 3D-printed object is illustrated in Figure 1. In the classical approach, a virtual model is obtained either through CAD software modeling or by using one of the methods applied in reverse engineering (such as 3D scanning, photogrammetry, coordinate measuring machines, etc.). Once the model is created, it is exported to a standard STL file, which is then processed in a slicer. The end result is a generated g-code file (for FFF/FDM technology), which is interpreted by the printer's processor to execute movements along the respective axes.

The diversity of 3D printing methods has made this technology – originally classified as a rapid prototyping method – widely applicable not only in engineering but also in scientific research, art, and education. Examples of engineering applications include the fabrication of complex geometric shapes for planar and spatial electronics solutions [12], or the printing of blades for small wind turbines [13]. An example of such additive technology applications in other fields is bioprinting in medicine [14]. Ferro et al. [15] are working on new structures made using SLM (selective laser melting) technology for anti-icing solutions

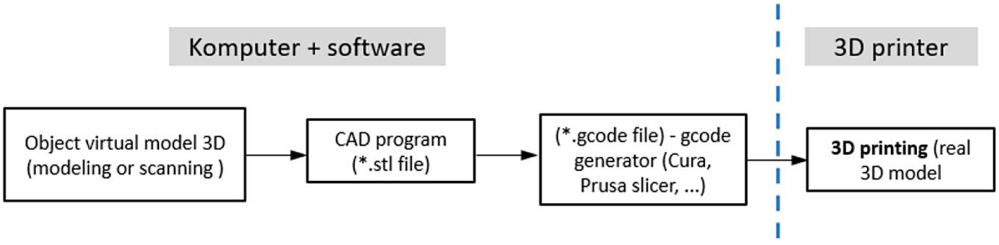

Figure 1. Flow chart of the process of making a real model using FFF/FDM additive technology - classical procedure

in aluminum. It is worth noting the emergence of studies on 4D printing [16], which involves materials that respond to external stimuli. Junk and colleagues have explored the possibility of printing grippers for specialized applications, in which the gripper closes as a result of temperature increase. Another branch of additive method development is the introduction of new types of materials. For instance, Kotorčević et al. [17] examined the use of PLA filament doped with copper for water filtration systems. Kujawa et al. [18] investigated the improvement of tribological and strength properties of PLA material doped with MoC2. They demonstrated an improvement in the quality of printed objects and an improvement in their resistance to external loads. Zubrzycki et al. [19] investigated the influence of printing parameters (layer height, temperature and printing speed) on the mechanical strength of samples made of ABS, PLA and PET-G materials.

To summarize, in every described case and development direction of additive manufacturing methods, users aim for the final printed part to be as accurate as possible compared to the CAD model - ensuring dimensional fidelity [1], minimizing print time, and maximizing the mechanical properties of the printed part, as achievable with the input material. These criteria often conflict with each other. For example, increasing the print speed (to reduce print time) increases vibrations in the printer, which can degrade print quality [2].

Meeting all of these criteria simultaneously is challenging, but continuous improvements are being explored. One such effort is the study by Liu et al. [20], in which the traveling salesman optimization method was used to reduce idle nozzle movements (i.e., non-extruding travel), thereby minimizing stringing effects that negatively affect print quality. On the other hand, Jadayel and Khameneifar [21] focused on improving print quality by modifying the STL file based on scans of a test print, without altering the g-code itself.

Artifical intelligence

Modern technological advancement is increasingly focused on implementing the principles of Industry 4.0. One of the most transformative tools in this context is artificial intelligence (AI), which is revolutionizing industrial processes [22]. AI offers a wide range of capabilities depending on how the neural network is designed by the programmer. It can, for example, predict undesirable events through real-time data monitoring using purpose-specific sensors. This can involve statistical analysis or image detection and interpretation.

Beyond monitoring and diagnostics, AI systems are capable of autonomous decision-making and initiating appropriate procedures in response to various situations. The most commonly used methods for such purposes include linear regression and decision trees. This reduces the level of human intervention in industrial processes, shifting the human role from primary operator to overseer, thereby minimizing human error. However, such applications require specialized knowledge in AI programming – typically using Python and libraries such as Keras, PyTorch, or TensorFlow.

Thanks to the development of large language models (LLMs) like ChatGPT, Gemini, or Copilot, even users with limited programming experience can now create specialized tools. This is done through the crafting of well-designed “prompts” – commands or instructions that guide the AI to carry out specific tasks. AI has also found its way into 3D printing, especially in areas related to machine learning for process diagnostics and monitoring. With properly trained algorithms, a 3D printer can autonomously detect issues such as:

- print detachment from the bed,
- stringing defects,
- inadequate nozzle temperature leading to inconsistent filament flow,
- clogged nozzles resulting in filament feed failure,
- filament depletion.

These issues can be detected using image analysis, which requires the integration of a camera with the printer to enable real-time image processing. Some companies have already implemented such solutions. For instance, Bambulab offers high-end printers that operate autonomously without requiring user intervention in the control system. In contrast, printers like the Ender 3 V3 Plus by Creality provide similar print speeds and quality, but integrating AI into these machines requires purchasing a compatible camera and having basic technical skills.

Creating an AI-based print monitoring and diagnostic system is possible for nearly any 3D printer equipped with a network interface. A Raspberry Pi microcontroller can be used to host a VPN server and process image data, though success may be limited by factors such as network latency, interruptions, or whether the

microcontroller's processor can handle AI algorithms, real-time image processing, and remote server operation simultaneously.

AI in 3D printing can be applied as early as the prototyping stage. Since the actual printing process is the final step in additive manufacturing, generative modeling offers an opportunity to design parts with optimized geometries that are difficult to achieve using traditional modeling methods – while still meeting mechanical strength requirements. This can reduce material use without compromising performance. In such cases, the user first creates a base shape, after which AI performs the optimization process.

This article also explores repeating the AI-assisted optimization at the next stage: converting the STL file to g-code. Since g-code is a sequence of machine instructions and functions as a programming language, it can be analyzed and modified like any other code – even by large language models like successive versions of ChatGPT. This practice is becoming increasingly common among both beginner and advanced developers.

This trend raises concerns about the potential impact on the job market, particularly for programmers who may be partially replaced by AI. The phenomenon – known as "prompt engineering" – is rapidly gaining traction and reshaping various long-standing professions. One could argue we are witnessing yet another industrial revolution.

Nvidia CEO Jensen Huang has even stated publicly that English is becoming one of the new programming languages – alongside Python, C, C#, C++, Java, and others [23]. While this was unthinkable until recently, the translation of human thought into code capable of generating or modifying professional-grade software is now increasingly achievable with each advancement in LLMs.

Advanced engineering software like MATLAB already supports custom script execution for analysis, simulation, and control across many technical fields. Large language models such as ChatGPT now have the capability to generate such scripts. Moreover, even if it's not yet possible to directly create a Simulink file (block-based graphical programming), AI can generate MATLAB scripts that, when run, build the desired block sequence programmatically.

MATERIALS AND METHODS

Among the many filaments available on the market, two widely used and readily accessible types were selected: Easy PLA [24] and Easy PET-G [25], both manufactured by Fiberlogy. For each of these filaments, the manufacturer provides essential printing parameters (such as temperature and mechanical), which are summarized in Table 1.

Slicing computer program

The samples for comparative testing were modeled in the Autodesk Fusion 360 environment. The resulting STL models were then sliced using Cura – a popular, free, and open-source software widely used by additive manufacturing enthusiasts. Cura enables the generation of g-code files for printers operating with FFF/FDM technology.

Cura offers more than 400 customizable settings, allowing for precise control over various aspects of the 3D model before printing. These include parameters such as layer height, infill, supports, wall thickness, cooling settings, and many others. The software integrates seamlessly with numerous popular CAD programs (e.g., SolidWorks, Autodesk Inventor), facilitating a smooth transition from design to print. Importantly, Cura is compatible with a wide range of file formats, including STL, OBJ, X3D, 3MF, BMP, GIF, JPG, and PNG. Another key advantage is its ability to import material profiles from leading filament manufacturers, streamlining the process of setting optimal print parameters.

Table 1. Printing and technical basic parameters of the tested filaments – data provided by the filament manufacturer. [24, 25]

Material	Nozzle temp. °C	Bed temp. °C	Airflow %	Print aver. mm/s
Easy PLA	200–230	50–70	75–100	<100
Easy PET-G	220–250	90	0–25	<100
Material	Density g/cm^3	Flexural modulus MPa	Flexural strength MPa	Tensile modulus MPa
Easy PLA	1.24	3800	81	3500
Easy PET-G	1.27	2000	70	2800

POINT BENDING STATION

The configuration of the measurement setup for testing the samples is shown in Figure 2. The components are labelled with the following numbers:

1. NEMA 57BYGH76 280 4a 4.25g stepper motor with a 4.25:1 gear ratio,
2. DM860H stepper motor driver,
3. Raspberry Pi 4,
4. HDMI LCD display,
5. Mechanism for converting rotary motion to linear motion using a TR8 trapezoidal threaded screw,
6. Manson NTP-5531 laboratory power supply,
7. Computer for data acquisition,
8. Arduino Uno R3,
9. SparkFun load cell amplifier,
10. Test sample compliant with ISO 14125,
11. NA27 strain gauge load cells.

To enable measurements on the constructed test stand, it is necessary to determine the quantities that allow for identifying the displacement of the element applying pressure to the samples. The analysis began by calculating the relationship between the number of motor steps, the gear ratio, and the lead screw pitch. The number of steps per rotation was calculated using Equation 1:

$$N_s = \frac{360^\circ}{angstep} = \frac{360^\circ}{1.8^\circ} = steps/rotation \quad (1)$$

where: $angstep = 1.80°$ – step angle of the NEMA 57BYGH76 stepper motor.

The displacement of the carriage Δx per one step of the stepper motor is calculated using Equation 2:

$$\Delta x = \frac{P}{N_s \times i} \quad (2)$$

where: $P = 8$ mm – lead of the TR8 trapezoidal screw, $i = 4.25$ – gear ratio.

After substituting the values, we obtain the displacement $\triangle x = 0.0094$ mm. The step constant was set in the motor driver to $\triangle t = 0.005$ s, which means the motor performs 200 steps per second (1 full rotation), resulting in the screw moving $200 \cdot \triangle x = 200 \cdot 0.0094 = 1.88$ mm/s. A key component enabling the determination of the fracture forces of the samples is the strain gauge beams used in the test stand. The basic parameters of the strain gauge beams are presented in Table 2.

In the case of the considered tests, the loading of the beams and the force measurement are performed in only one direction (Figure 3a). Hysteresis error becomes significant in measurements where the deformation of the beams and the readings would be carried out bidirectionally (Figure 3b).

The repeatability coefficient was verified by repeatedly performing measurements involving

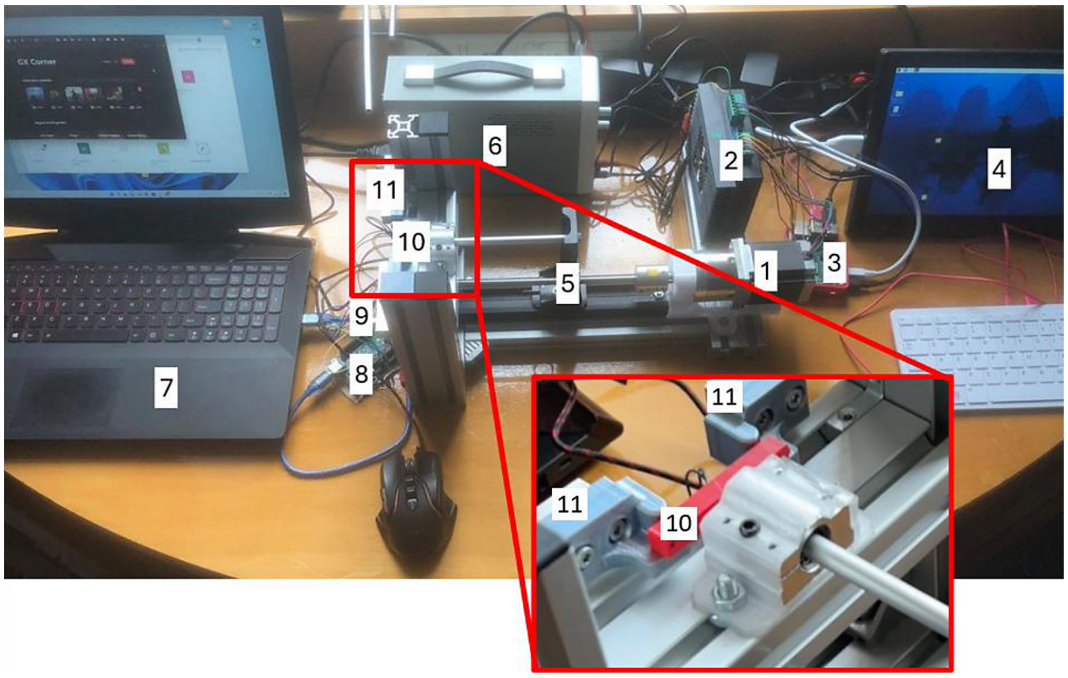

Figure 2. Station for testing the strength of printed samples

Table 2. Basic parameters of the NA27 strain gauge beams, with dimensions 80 × 13× 13 mm, used in the measurement system

Measure range N	non-linearity %F.S.	Hysteresis %F.S.	Repeatability %F.S.
100	0.03	0.03	0.03

an increase in the applied force followed by its return to a value close to 0 N. This approach allows for demonstrating the accuracy with which the force increases as a function of the sample's displacement. The results of the recorded measurements for both increasing and decreasing force values are presented in Figure 4. The area corresponding to force increase, marked with a frame, represents the sample fracture experiment (Figure 3).

Subsequently, the Type A uncertainty was determined (this type of uncertainty is calculated based on measurements).To determine it, the arithmetic mean of the performed measurements must be calculated according to the following formula:

$$\bar{x} = \frac{1}{n}\sum_{i=1}^{n} x_i \tag{3}$$

where: $n = 4$ – number of trials, x_i – value of the measurement in the i-th trial.

Based on the arithmetic mean (Eq. (3)), the standard deviation is calculated as follows [26]:

$$s = \sqrt{\frac{1}{n(n-1)}\sum_{i=1}^{n}(x_i - \bar{x})^2} \tag{4}$$

Finally, the Type A uncertainty (standard uncertainty of the mean) is calculated using Equation 5:

$$u_A = \frac{s}{\sqrt{n}} \tag{5}$$

The result of this experiment in the form of a measurement table (shown for example for the

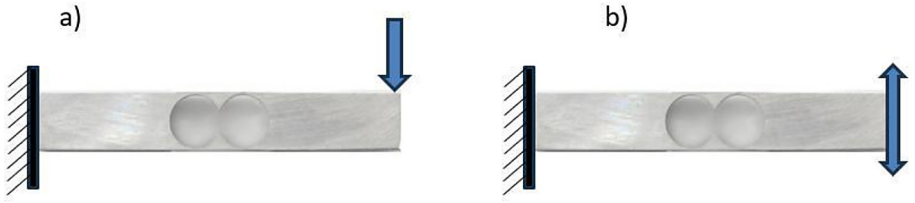

Figure 3. Loading variants of the measurement beams: (a) unidirectional loading variant, (b) bidirectional loading variant

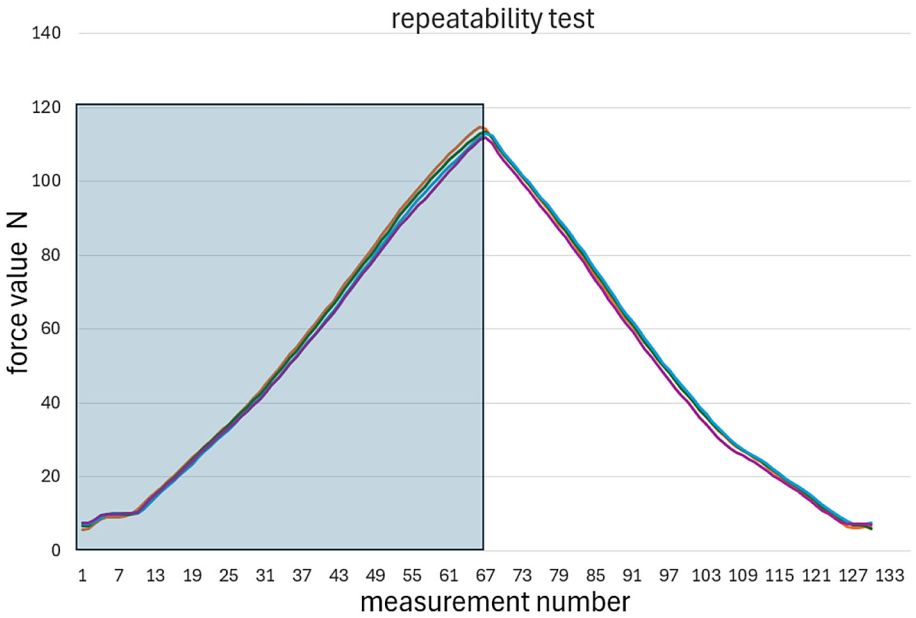

Figure 4. Results of the four performed loading tests of the strain gauge beams

first 5 measurements out of 68 recorded for each trial) is presented in Table 3.

Based on the 4 conducted trials, in which 68 measurements were recorded for each trial within the force increase range up to a maximum of 112 N (see Figure 4), the Type A measurement uncertainty and its mean value were estimated. The results are presented in Figure 5.

Samples for testing

For the testing of reference samples (unmodified by the AI algorithm) and modified samples, test stands for three-point bending tests were used in accordance with ISO 14125. According to this standard, the samples should have dimensions of L = 80 mm, b = 10 mm, and h = 4 mm. The standard also allows for samples with other dimensions. The shape of the sample used for testing is shown in Figure 6.

Basic gcode modified with AI

The proposed modified procedure involves the use of artificial intelligence algorithms to optimize the G-code in order to achieve a noticeable improvement in a selected parameter of the 3D printing process. This may include, for example, an enhancement of the mechanical strength of the print or an improvement in the printing process itself (e.g., shortening the print time without compromising quality). Figure 1 presents a schematic of the traditional model preparation workflow for a 3D printer.

The proposed workflow incorporating AI-based G-code modification is shown in Figure 7. Creation of a specialized thread in the large language model Chat GPT-4o (Omni), primarily intended for advanced operations that are not so much creative as technical and engineering-oriented [27].

Table 3. Results of the first 5 measurements in each of the 4 trials, along with the arithmetic mean, standard deviation, and Type A uncertainty

Probe					x	s	u_A
Measurements	1	2	3	4			
1	5.7	6.7	7.4	7.5	6.83	0.42	0.21
2	6.1	6.9	7.4	7.9	7.0	0.33	0.17
3	7.3	7.7	7.8	8.4	7.8	0.23	0.11
4	8.6	9.0	8.9	9.6	9.03	0.21	0.10
5	9.0	9.8	9.9	10.0	9.68	0.23	0.11

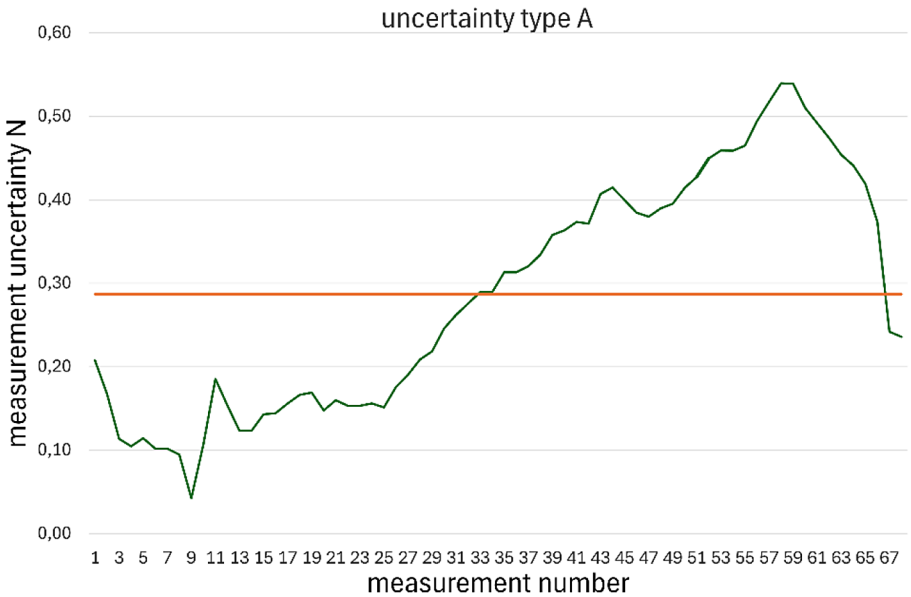

Figure 5. The value of the Type A measurement uncertainty and its mean. The mean uncertainty within this range of force variation is 0.29 N

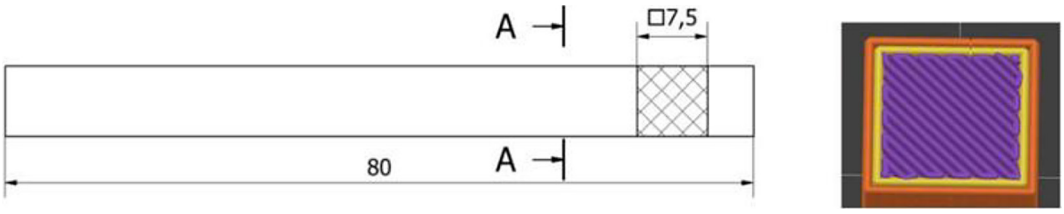

Figure 6. Shape of the sample used in the measurements

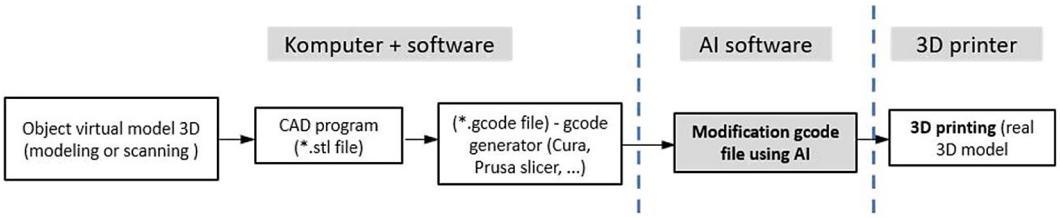

Figure 7. Process diagram for manufacturing a physical model using additive FFF/FDM technology – procedure including G-code modification by an AI algorithm

The content of the prepared prompt is presented below.

Creation of a specialized thread in the large language model Chat GPT-4o (Omni), primarily for advanced tasks that are more technical and engineering-focused rather than creative [27]. The content of the prepared prompt is presented below: "Hello, please assume the role of a 3D printing specialist. You specialize in modifying existing G-code programs. This thread of conversation concerns the modification of existing G-code. I am focused on increasing the strength of the prints. I cannot afford to increase the number of walls or the infill density or change the infill pattern. I am attaching the datasheet of my 3D printer and the datasheet of the filament I plan to use. Please optimize the G-code by modifying the speeds and temperatures used. Apply changes to every second or third layer in terms of speed and temperature to achieve the best possible strength results. I will be asking you to modify the G-code file that I will provide. Please refer only to scientifically proven optimization assumptions and information obtained through the analysis of the attached datasheets".

1. Polite greeting – interestingly, it has been observed that when users of AI language models politely address the model as a conversation partner, better results are often achieved. Although this is somewhat concerning, it is understandable given the immersive nature of the interaction.
2. Specialization enforcement – at this point, the scope of the thread is deliberately limited to a non-creative context. By instructing the model to act as a specialist in the relevant discipline, the user ensures a higher likelihood of receiving accurate and technically grounded responses. The GPT-4o model was chosen for this scenario as it is particularly suited for technical tasks.
3. Task specification – this is the most crucial part of the prompt. The language model is given a specific task along with a clear role definition. Without such a directive, the model is more prone to error due to a lack of context and role awareness.
4. References and input constraints – another critical instruction. The language model may have been trained on data concerning typical 3D printing materials such as PLA, PETG, or ABS. However, each filament may have different optimal parameters depending on the manufacturer, properties, or even color. By requiring the model to refer to actual datasheets, the user ensures that the algorithm bases its modifications on verified data related to both the filament and the printer – two key components of the FFF/FDM process.
5. Task refinement – this functions as a reiteration of the task but with more detail. It specifies the exact type of modifications the user expects. Repeating the task (even multiple times) is important in prompt engineering, as it improves the model's "understanding" of the desired output. Just like neural networks are trained through layers and input weighting, repeated instruction functions as additional learning

reinforcement for the thread.

6. Reiteration of constraints – as mentioned, this serves as another safeguard layer. It ensures the creative module is suppressed. While creativity is beneficial in marketing content, in this technical context it poses a risk of generating misleading or even hazardous instructions for the printer. Referring only to scientific, validated modifications serves as a solid protection mechanism in the training of the model's behavior.

In the described case (Figure 8), traditional programming languages such as Python are not used. Instead, a linguistic model is applied by accurately and consciously formulating specific commands using natural human language—moreover, in almost any language. This is particularly significant as it eliminates limitations caused by language barriers, creating new opportunities for programming artificial intelligence for a much broader audience, not necessarily English-speaking.

RESULTS

The results of the conducted measurement experiments are presented in the following subsections in the form of graphs showing the increase in force from the moment the test stand is activated until the maximum force is reached at the point of breakage (sample deformation). The experiments were carried out using samples with dimensions of 100 × 7.5 × 7.5 mm, which are approved for testing according to the ISO 14125 standard. A greater sample height of 7.5 mm was selected (the standard height is 4 mm) to allow for more print layers, and thus more opportunities to change the printing parameters. For this chosen sample shape, three types of specimens were produced: original ones (without any modification of the g-code generated in the CURA software), specimens modified every 2 layers, and specimens modified every 3 layers. The tests were conducted on samples made of Easy PLA [24] and Easy PET-G [25] from Fiberlogy. These variants are referred to in the further sections as follows:

- NMP – samples without g-code modification,
- PM2L – samples with g-code modified every 2 layers,
- PM3L – samples with g-code modified every 3 layers.

Results for samples with a dimension of 100 × 7.5 × 7.5 mm – Easy PLA material

For these sample dimensions, measurements were carried out on 10 specimens for each variant. Figure 9 presents the results obtained for samples printed using unmodified g-codes generated by slicers (NMP), samples modified every 2 layers (PM2L), and samples modified every 3 layers (PM3L). The values for each of the tests are illustrated in Figure 9 and the maximum values of the breaking force are summarized in Table 4. The cases NMP, PM2L and PM3L presented in the figure represent the time histories of the increase in force measured on the tensometric beams (the places where the samples were supported – see Figure 2). For each of the cases, 10 tests were performed and summarized in the figure. The maximum values corresponding to the moment of sample fracture are summarized in

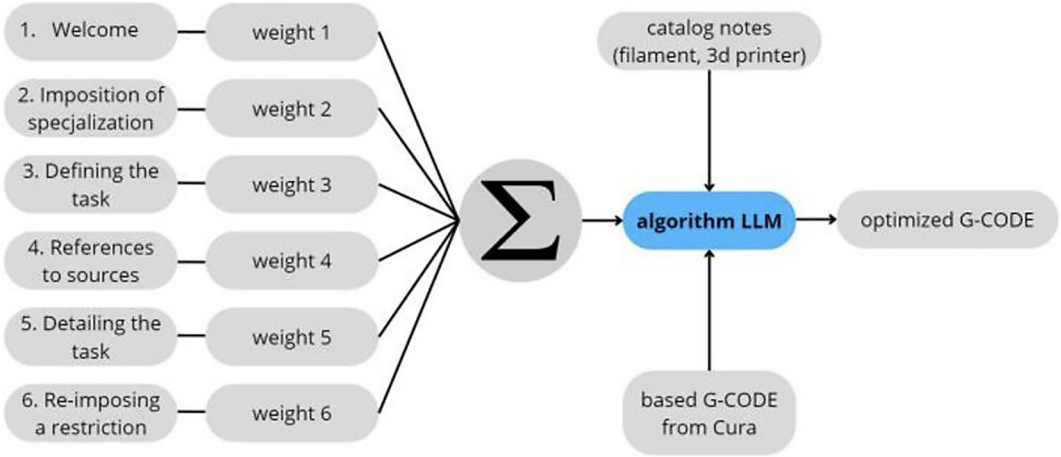

Figure 8. Diagram of the AI prompt formulation process

Table 4 and then the average value was calculated from the 10 maximum values (F_{avg} in Table 4).

The increase in the breaking force of the Easy PLA samples based on AI-modified g-code files (PM2L) compared to the baseline samples (NMP) is just under 2.7%. The percentage difference in breaking force for samples modified every 3 layers (PM3L) relative to the NMP samples is just under 3.0%. The time histories of the force increase shown in Figure 9 demonstrate the specificity of the PLA material. It consists in the fact that the samples transfer the load exerted in their central part to the supports until the limit value of the force is reached and then the samples break, which is manifested in the histories by a sudden drop in the force to 0.

Results for samples with a dimension of 100 × 7.5 × 7.5 mm – Easy PET-G material

For these sample dimensions, measurements were conducted on 10 specimens for each variant. Figure 10 presents the results obtained for samples printed using unmodified g-codes (generated by slicers – NMP), samples modified every 2 layers (PM2L), and samples modified every 3 layers (PM3L). All samples were made from Easy PET-G using filament from a single spool. The values for each of the tests are illustrated in Figure 10 and the maximum values of the breaking force are summarized in Table 5. For each of the cases, 10 tests were performed and summarized in the figure. The maximum values corresponding to the moment of sample fracture are summarized in Table 5 and then the average value was calculated from the 10 maximum values (F_{avg} in Table 5).

The increase in the breaking force of the Easy PET-G samples based on AI-modified g-code files (PM2L) compared to the baseline samples (NMP) is just under 4.3%. The percentage difference in breaking force for samples modified every 3 layers (PM3L) relative to the NMP samples exceeds 9.9%. The time courses of force increase shown in Figure 10 show the specificity of the PET-G material. It consists in the fact that the samples transfer the load exerted in their central part to the supports until the limit value of the force is reached and then the samples undergo plastic deformation – which is visible in the part of the course after the maximum value. The force does not decrease to 0

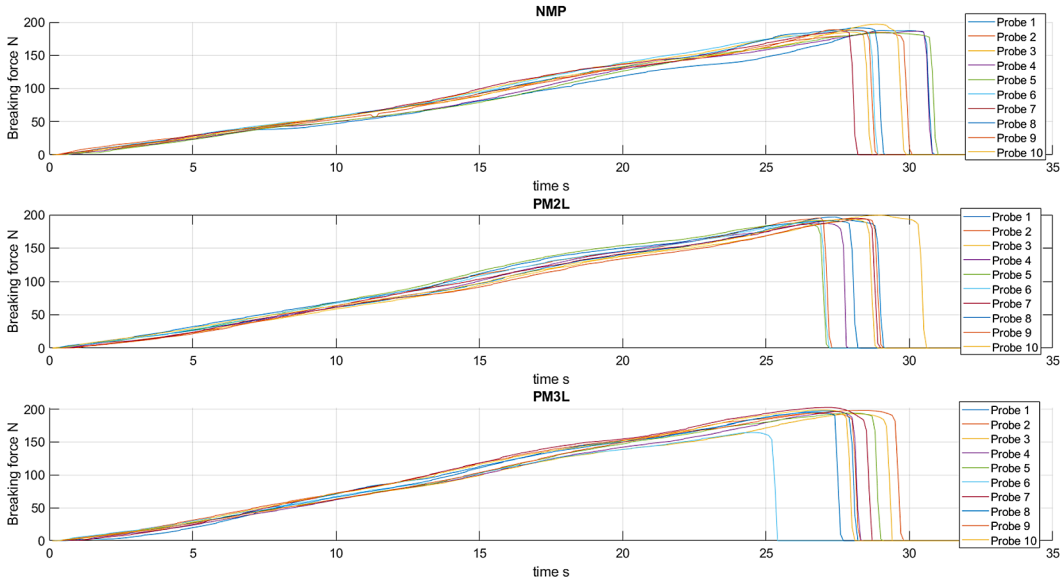

Figure 9. Measurement results obtained for the baseline samples (NMP) and the samples modified every 2 layers (PM2L) and every 3 layers (PM3L) using Easy PLA material

Table 4. Maximum values for the measurements conducted on the baseline samples (NMP) and the samples modified every 2 layers (PM2L) and every 3 layers (PM3L) made from Easy PLA material

Pr.	1	2	3	4	5	6	7	8	9	10	F_{avg} N
NMP	187.3	185.0	184.8	186.4	184.1	187.0	186.3	191.2	188.6	196.9	187.76
PM2L	196.8	195.0	199.4	187.4	187.4	189.1	194.7	191.0	193.6	193.3	192.76
PM3L	197.3	193.5	192.8	196.2	194.4	164.7	202.7	195.2	197.9	198.7	193.34

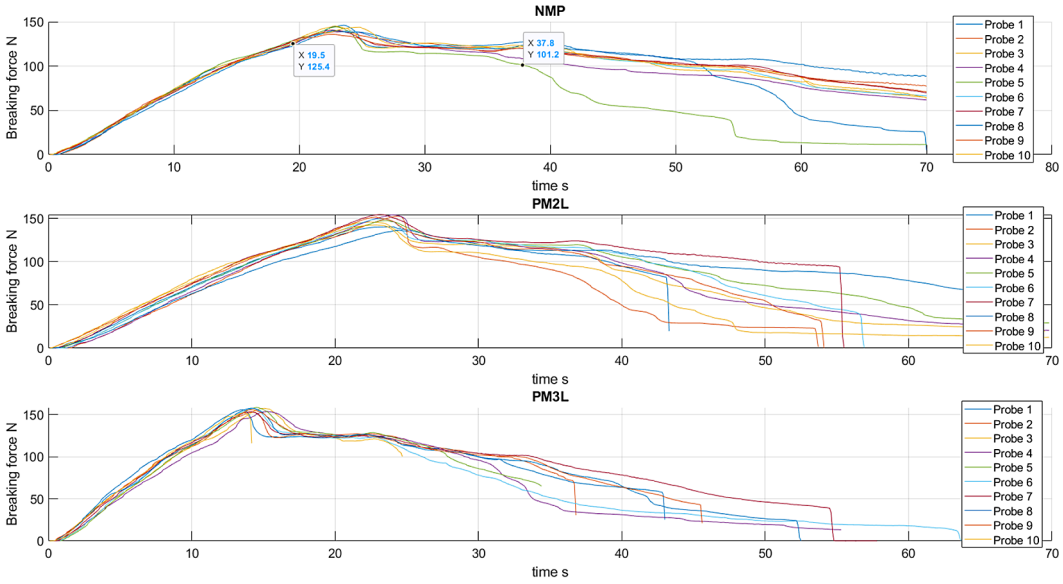

Figure 10. Measurement results obtained for the baseline samples (NMP) and the samples modified every 2 layers (PM2L) and every 3 layers (PM3L) made from Easy PET-G material

Table 5. Maximum values for the measurements conducted on the baseline samples (NMP) and the samples modified every 2 layers (PM2L) and every 3 layers (PM3L) made from Easy PET-G material

Pr.	1	2	3	4	5	6	7	8	9	10	F_{avg} N
NMP	146.1	139.6	145.3	139.5	144.3	139.7	140.8	140.2	135.9	143.8	141.52
PM2L	140.4	152.7	145.9	154.2	147.6	148.6	154.5	136.5	151.7	142.6	147.57
PM3L	155.9	153.0	157.6	153.8	158.6	157.3	153.5	157.8	155.8	152.2	155.55

Table 6. Values of key parameters extracted from the g-code files CE3_1.gcode, CE3_2.gcode, and CE3_3.gcode

Parameter/commandS	CE3_1.GCODE (CURA – ORIGINAL)	CE3_2.GCODE CHATGPT-4	CE3_3.GCODE CHATGPT-4O
Total lines	4058	4112	4112
G1 – controlled linear movement with optional extrusion	1697	1697	1724
G0 – fast linear movement without material extrusion	2120	2120	2120
G92 – setting current position as reference point	4	4	4
G28 – automatic positioning to zero position	1	1	1
M104 – number of commands setting the hotend temperature (without waiting)	3	30	30
M109 – number of commands setting the hotend temperature (with waiting)	1	1	1
M106 – enable cooling fan	4	4	4
M107 – disable cooling fan	2	2	2
M140 – setting bed temperature without waiting	3	3	3
M190 – setting bed temperature with waiting until reached	1	1	1
Comments	212	212	212
Z movements	36	36	36
X movements	3801	3801	3801
Y movements	3801	3801	3801
E movements – extruder position	1689	1689	1689
F (feedrate) – movement speed	2472	2472	2499
Layer changes layer change comments	27	27	27

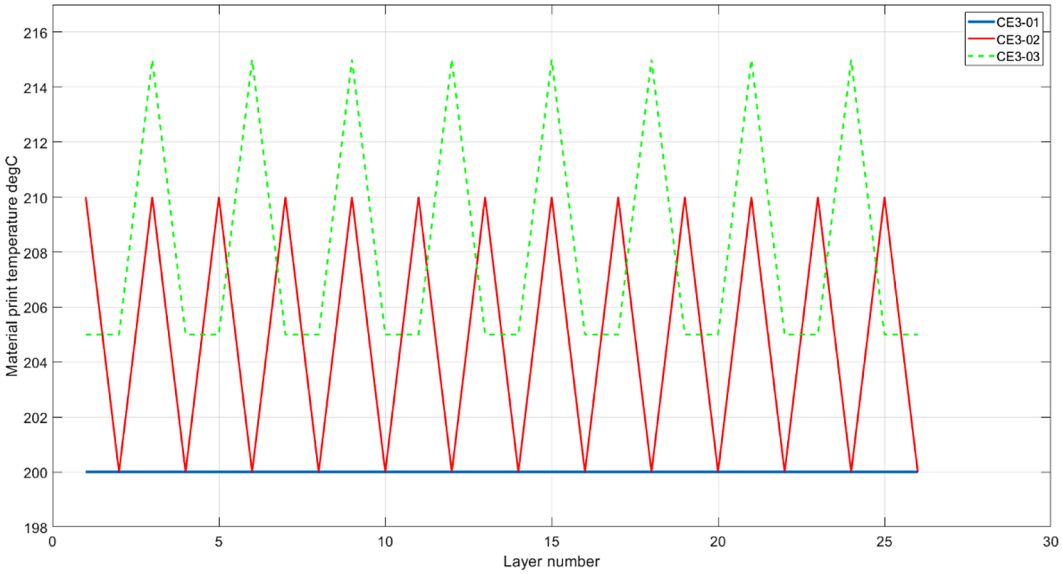

Figure 11. Temperature values extracted from the g-code files CE3_1.gcode, CE3_2.gcode, and CE3_3.gcode

(the moment of sample fracture) as in the case of samples made of PLA material. PET-G samples start to deform but do not break brittle.

G-CODE files for 100 × 7.5 × 7.5 samples (PM2L) – Easy PLA material, before and after modification

Printing parameters (nozzle temperature) were compared – Table 6 and Figure 11. Table 6 lists the key commands saved in the g-code file, respectively: CE3_1.gcode – file generated by the CURA slicer, CE3_2.gcode – file generated by the CURA slicer and modified by ChatGPT-4 in June 2024, and the CE3_3.gcode file – file generated by the CURA slicer and modified by ChatGPT-4o after a year in May 2025. As shown in previous chapters, g-code modifications due to temperature changes during printing have a measurable effect on the strength of samples tested using the three-point bending method. Figure 11 shows the temperature changes specified in the g-code files CE3_1.gcode, CE3_2.gcode, and CE3_3.gcode.

CONCLUSIONS

The conducted research demonstrated that the application of artificial intelligence algorithms to optimize g-code files used in fused filament fabrication (FFF/FDM) 3D printing technology yields measurable benefits in terms of improved mechanical performance of printed objects. Modifying g-code files using the ChatGPT-4o language model led to a 2.7% increase in average breaking force for Easy PLA samples when temperature was modified every 2 layers, and a 3.0% increase when modified every 3 layers. Even more significant improvements were recorded for Easy PET-G, with a 4.3% increase in average breaking force for modifications every 2 layers and a 9.9% increase for every 3 layers.

These results indicate a material-dependent response to AI-based optimization: Easy PET-G exhibited nearly 3 times greater strength gain in the PM3L variant than Easy PLA, likely due to its wider optimal processing temperature range (220–250 °C vs. 200–230 °C) and higher thermal responsiveness. The proposed method, relying on large language models for g-code modification, is both technically accessible and effective, requiring only a properly formulated prompt and knowledge of the printer and filament specifications.

Comparative analysis of the g-code files revealed that the AI-generated modifications increased the number of M104 commands (hotend temperature setting) from 3 in the baseline file to 30, introducing cyclic thermal adjustments that likely improved interlayer bonding. Additionally, the number of G1 commands increased slightly (from 1697 to 1724), indicating minor adjustments to the extrusion path, and F values (feedrate commands) were modified (from 2472 to 2499 entries), suggesting targeted optimization of movement speeds.

This research confirms that AI-assisted g-code editing can lead to quantifiable improvements in 3D printed part strength without altering geometry, increasing material use, or requiring hardware modifications. The method shows promise for broader application, particularly within Industry 4.0 paradigms, where automated process optimization is highly valued.

REFERENCES

1. Jałowiec, M., Walcher, E.-M., Bodur, O., Poszvek, G., Klein, M., Bayrakçıl, M.D. Advanced quality assurance of additive manufacturing through computed tomog-raphy. In: Durakbasa, N.M., Gençyılmaz, M.G. (eds.) Industrial Engineering in the Industry 4.0 Era, Springer, Cham 2024; 179–199.
2. Pilch, Z., Domin, J., Szłapa, A. The impact of vibration of the 3d printer table on the quality of print. In: WZEE'2015, 2015; 147–152.
3. Vaezi, M., Seitz, H., Yang, S. A review on 3d micro-additive manufacturing technologies. International Journal of Advanced Manufacturing Technology 2013; 67(5–8), 1721–1754.
4. Pandey, P.M., Reddy, N.V., Dhande, S.G. Real time adaptive slicing for fused deposition modelling. International Journal of Machine Tools and Manufacture 2003; 43(1), 61–71.
5. Sala, R., Regondi, S., Pugliese, R. Design data and finite element analysis of 3d printed poly-caprolactone-based lattice scaffolds: Influence of type of unit cell, porosity, and nozzle diameter on the mechanical behavior. Eng 2022; 3(1): 9–23. https://doi.org/10.3390/eng3010002
6. Özen, A., Auhl, D., Völlmecke, C., Kiendl, J., Abali, B.E. Optimization of manufacturing parameters and tensile specimen geometry for fused deposition modeling (fdm) 3d-printed petg. Materials 2021; 14(10). https://doi.org/10. 3390/ma14102556
7. Tichý, T., Šefl, O., Veselý, P., Dušek, K., Bušek, D. Mathematical modelling of temperature distribution in selected parts of fff printer during 3d printing process. Polymers 2021; 13(23). https://doi.org/10.3390/polym13234213
8. Cacace, J., Finzi, A., V., L. A grasping simulator for informed grasp planning based on visual data. In: Proceedings of the IEEE/RSJ International Conference on Intelligent Robots and Systems (IROS), 2016; 1177–1183.
9. Wang, J., Zheng, P., Xu, X. An artificial intelligence-based process planning framework for smart manufacturing. Journal of Manufacturing Systems 2020; 54, 328– 340.
10. Mueller, T., Koch, R. Ai-based optimization for additive manufacturing. Proce-dia CIRP 2020; 88, 279–284.
11. Bellini, A., Güçeri, S.: Mechanical characterization of parts fabricated using fused deposition modeling. Rapid Prototyping Journal 2003; 9(4), 252–264. https://doi.org/10.1108/13552540310489631
12. Macdonald, E., Salas, R., et al. 3d printing for the rapid prototyping of structural electronics. IEEE Access (2014) https://doi.org/10.1109/ACCESS.2014.2311810. Received February 14, 2014, accepted March 1, 2014, date of publication March 13, 2014, date of current version April 7, 2014
13. Poole, S., Phillips, R. Rapid prototyping of small wind turbine blades using additive manufacturing. In: 2015 Pattern Recognition Association of South Africa and Robotics and Mechatronics International Conference (PRASA-RobMech), Port Elizabeth, South Africa, 2015; 189–194. https://doi.org/10.1109/RoboMech. 2015.7359521
14. Tack, P., Victor, J., et al. 3d-printing techniques in a medical setting: a system-atic literature review. BioMedical Engineering OnLine 2016. https://doi.org/10. 1186/s12938âĂŚ016âĂŚ0236âĂŚ4
15. Ferro, C.G., Varetti, S., Maggiore, P.: Experimental evaluation of mechanical compression properties of aluminum alloy lattice trusses for anti-ice system applications. Machines 2024; 12(6). https://doi.org/10.3390/machines12060404
16. Junk, S., Einloth, H., Velten, D. 4d printing: A methodical approach to product development using smart materials. Machines 2023; 11(11). https://doi.org/10. 3390/machines11111035
17. Kotorčević, N., Milenković, S., Živić, F., Jordović, B., Adamović, D., Todorović, P., Grujović, N.: Material extrusion 3d printing of micro-porous copper-based structure for water filters. Machines 2024; 12(7). https://doi.org/10.3390/ machines12070470
18. Kujawa, M., Głowacka, J., Pawlak, W., Sztorch, B., Pakuła, D., Frydrych, M., Sokolska, J., Przekop, R.E. Molybdenum disulphide modified polylactide for 3D Printed (FDM/FFF) filaments. Polymers 2023, 15, 2236. https://doi.org/10.3390/polym15102236
19. Zubrzycki, J., Quirino, E., Staniszewski, M., Marchewka, T. Influence of 3D printing parameters by FDM method on the mechanical properties of manufactured parts. Advances in Science and Technology Research Journal, 2022; 16(6), 356–366. https://doi.org/10.12913/22998624/154024
20. Liu, H., Liu, R., Liu, Z., Xu, S. Minimizing the number of transitions of 3d printing nozzles using a traveling-salesman-problem optimization model. Inter-national Journal of Precision Engineering and Manufacturing 2021; 22(6), 1617–1637. https://doi.org/10.1007/s12541-021-00512-2
21. Jadayel, M., Khameneifar, F. Improving geometric accuracy of 3d printed parts using 3d metrology feedback and mesh morphing. Journal of Manufacturing and Materials Processing 2020; 4(4). https://

doi.org/10.3390/jmmp4040112

22. Bonada, F., Echeverria, L., Domingo, X., Anzaldi, G. Ai for improving the overall equipment efficiency in manufacturing industry. In: Martínez, L.R., Rios, R.A.O., Prieto, M.D. (Eds.) New Trends in the Use of Artificial Intelligence for the Industry 4.0. IntechOpen, Rijeka (2020). Chap. 5. https://doi.org/10.5772/intechopen.89967
23. Nvidia: Children Will No Longer Need To Learn To Code. https://www.educationnext.in/posts/children-will-no-longer-need-to-learn-to-code-nvidia-ceo-jensen-huang. Dostęp: 13 października 2024, 2024.
24. Fiberlogy: Easy PLA filament. https://fiberlogy.com/pl/filamenty/filament-easy-pla/. Dostęp: 19 lipca 2024, 2024.
25. Fiberlogy: Easy PET-G filament. https://fiberlogy.com/pl/filamenty/easy-pet-g/. Dostęp: 19 lipca 2024, 2024.
26. Ratcliffe, C., Ratcliffe, B.: Type A and Type B Elemental Uncertainties, Springer, Cham 2015; 9–18. https://doi.org/10.1007/978-3-319-12063-8_2 . https: //doi.org/10.1007/978-3-319-12063-8_2
27. Aljanabi, M., Yaseen, M.G., Ali, A.H., Mohammed, M.A. Prompt engineering: Guiding the way to effective large language models. Iraqi Journal for Computer Science and Mathematics 2023.